80N22331

QCGAT AIRCRAFT/ENGINE DESIGN FOR REDUCED
NOISE AND EMISSIONS

Leonard I'Anson and Kenneth M. Terrill
Avco Lycoming Division

INTRODUCTION

The multi-engine general aviation fleet size is expected to increase by 70 percent in the decade of the 1980's according to the General Aviation Manufacturers Association (GAMA). These general aviation aircraft typically use suburban airports that are unprotected by commercial buffer zones. Consequently, there is the potential for general aviation to create more widespread adverse community reaction to noise and pollution than that experienced with commercial air carrier aircraft. Recognizing this, NASA let contracts to apply large engine quieting and emissions reduction technology to smaller engines and to develop new and more suitable technology where required. These resulting "Quiet, Clean, General Aviation Turbofan" (QCGAT) contracts required delivery of a turbofan engine and nacelle demonstrator, as well as preliminary defintion of an appropriate general aviation aircraft system, that could use the engine as propulsion.

This paper describes the resulting aircraft/nacelle/engine designs created under the Avco Lycoming contract. These designs reflect the technical expertise of the following subcontractors:

> Aircraft Design - Beech Aircraft Corporation
> Nacelle Mechanical Design - Avco Aerostructures
> Nacelle Acoustic Treatment - Lockheed Aircraft Corporation

AIRCRAFT PRELIMINARY DESIGN

To guide the aircraft system design, five primary objectives were established:

1. Practical, direct application of technology without significant scaling was very important. This required selection of aircraft and engine sizes which would be appropriate for an appreciable segment of general aviation.

2. The aircraft must also offer attractive range, fuel economy, and flight speed. A target of 2593 kilometers (1400 nautical miles) was established. This exceeds the range of most current small business aircraft. It also provides non-stop travel between opposite extremes of high density traffic areas.

3. A cruise Mach Number of 0.62 was chosen as an optimum compromise between time and fuel economy. It provides 40 percent higher cruise speed than a turboprop, with a 30 percent improvement in fuel economy over operation at 0.8 Mach Number.

4. A balanced field length of 762 meters (2500 feet) was desired because it permits safe operation from 70 percent of all U.S. airports which are open to the public, including airports with sod runways.

5. Ecological characteristics of an aircraft system are likely to become primary competitive parameters for general viation in the 1980 decade. Therefore, they deserve close attention in design selections.

The initial step in aircraft preliminary design was the selection of appropriate size and design. The vast majority of general aviation aircraft operating from airfields located in suburban communities are in the size class below 5433 kg (12,000 lb) gross weight. In the lower extremity of the gross weight spectrum, small private aircraft in the range below 1814 kg (4,000 lb) are generally powered by single-piston engines. It is expected that market constraints for very low-cost aircraft in this class will dictate continued usage of piston engines for the foreseeable future. It, therefore, follows that the greatest public ecological benefits can be realized by introduction of a quiet, clean aircraft system in the 1814 - 5433 kg (4,000 - 12,000 lb) gross weight class. Figure 1 shoes the projected market volume for various sizes of general aviation aircraft.

As with the passenger car trend towards smaller and more sophisticated cars to perform the same function, it is expected that the decade of 1980's will see a similar general aviation trend towards reduced aircraft weight and smaller engine size for the same mission. Because noise, emissions, and fuel consumption reduce with engine size, subsequent improvement in ecological characteristics can be anticipated. Utilizing technologies such as turbofan propulsion, high aspect ratio super critical wing and lightweight composite structures, it is expected that a new class of small general aviation aircraft will emerge in the eighties. A target of 30 percent weight reduction was considered achievable.

For aircraft size selection, our target was the largest segment of general aviation aircraft where cost of turbofan propulsion does not preclude its introduction.

Figure 1 presents a composite plot of aircraft gross weight versus both "The Number of New Aircraft to be Built" and "The Current Estimated Nominal Aircraft Cost". The number of aircraft is based on General Aviation Manufacturers Association data. The expected trend toward lighter weight and higher cost for the same mission has not been reflected to ensure conservative engine sizing. The range of 3175 - 4536 kg (7,000 to 10,000 lb) gross weight appeared attractive, with 3629 kg (8,000 lb) selected as our goal.

With the defined aircraft goals and Lycoming estimates for engine performance, Beech Aircraft Corporation conducted parametric studies to optimize the aircraft preliminary design.

The aircraft which evolved is depicted in figure 2. It is a sleek, advanced design, six-place aircraft with 3538 kg (7,800 lb) maximum gross weight. It offers a 2778 kilometer (1500 nautical mile) range with cruise speed of 0.5 Mach Number and will take-off and land on the vast majority of general aviation airfields. Advanced features include broad application of composite materials and a supercritical wing design with winglets. Full-span fowler flaps have been introduced to improve landing capability. Engines are fuselage-mounted with inlets over the wing to provide shielding of fan noise by the wing surfaces.

The high bypass ratio QCGAT engine plays an important role in shaping the aircraft design. It offers a dramatic reduction in specific fuel consumption compared with current pure jets and low-to-moderate bypass ratio turbofans. Figure 3 provides this comparison, reflecting a 22 percent improvement in fuel economy.

This lower fuel consumption may be used in either of two ways or in combination:

It can substantially reduce aircraft gross weight for the same range. The reduced weight provides compound interest on the fuel economy. It also requires lower thrust favoring reduction of noise and emissions.

If preferred, the lower fuel consumption can be translated into longer range for the original gross weight.

We chose to reduce gross weight and favor ecological characteristics.

Composite structures have been used extensively in the aircraft preliminary design to further reduce gross weight. Areas selected by Beech for the application of composite materials are shown in figure 4. Kevlar graphite composites were used for aircraft weight estimates. Further potential for weight savings exists in the engine nacelles. Conventional design was used to reflect the low-risk, low-cost test nacelle. Critical load carrying members such as the wing spar are conventional aluminum construction.

Approximately 40 percent of the structure is fiber epoxy or honeycomb-bonded structure. The use of composite structure in aircraft design provides a decreasing rate of benefit as the application of composites becomes more widespread in the design. Initial selection of applications is in noncritical areas. As the stress in selected areas increases, the design safety factor also increases to compensate for uncertainties resulting from the youth of the composite application. Beech cautions that, while these composite applications are technically feasible, development beyond the scope normally undertaken by industry would be required to assure success.

Structural design is in accordance with Federal Aviation Regulation Part 23 airworthiness standards for normal category airplanes.

A 17 percent thickness-to-chord ratio supercritical wing shape was selected because it offers a number of advantages over the conventional 12 percent NACA shape. These advantages are summarized in figure 5.

> From the cross sectional comparison shown here, it can be concluded that the supercritical wing provides larger volume for fuel storage for the same chord width. The thickness increase has the supplementary benefit of higher section modulus, permitting lighter construction for equivalent bending loads.

> The two shapes have comparable drag characteristics in the cruise mode. Increase in the NACA airfoil thickness in an attempt to achieve similar volume is impractical, because it results in a significant reduction in useful flight speed combined with an overall drag increase at lower speeds.

> Iterative design studies show a 25 percent increase in fuel capacity combined with a 3 percent decrease in aircraft gross weight. These savings are for an equivalent aspect ratio of 10 and a design wing loading of 2250 N/m^2 (47 lb/sq ft) of wing area.

> Prior test data have shown an appreciable increase in lift capability as depicted in this comparison. This promises a more forgiving aircraft for variations in angle of attack, enhancing safety. For equivalent sophistication of flap systems, reduced landing speeds are achievable resulting in shorter landing field length capability.

The airfoil selected by Beech is similar to the NASA GA (W) - 1 airfoil, but is tailored specifically for the high-speed, high fuel volume and the high-lift requirements of the QCGAT configuration. The pressure distribution used to guide the design tailoring would identify it as a BAC Sonic Plateau airfoil with a 17 percent thickness ratio.

Full-span fowler flaps and spoilers have been introduced to achieve the desired 762 meter (2500 feet) take-off field length and landing distances with reduced wing area. Winglets have also been added to reduce actual span and wing structural weight, while maintaining high effective aspect ratio.

Major lift parameters are summarized below. Establishing optimum flap settings was beyond the scope of this study. However, experience indicates that a full flap deflection of 40 degrees for landing and take-off flap setting of 40 percent of full deflection are appropriate for fowler flap design. These values of $C_{L_{max}}$ represent available state-of-the-art with advanced airfoils.

Flap Positions	C_L @ = 0	$\dfrac{d\,C_L}{d}$	$C_{L_{max}}$
Up	.132	.088	1.6
40% (Take-Off)	.98	.088	2.35
Down	2.13	.088	3.45

Many drag influencing design details of the QCGAT airplane are not established at this time, because the airplane is as yet a preliminary design study. For drag analysis, ambitious estimates were made for the various items. Achievement of total airplane drag coefficients will require exacting effort in the practical development of the airplane. The resulting QCGAT aircraft drag compares with that of the Learjet Model 24, which is an extremely clean airplane. Allowances have been made for differences in wing thickness, component sizes, etc. Drag coefficients used are summarized below:

Total C_{D_p}, Flaps and gear up   .02661, .02534 cruise

Incremental C_{D_p} for landing gear   .0164

Incremental C_{D_p} for full flap   .04066

Incremental C_{D_p} for T.O. flap   .0163

Incremental C_{D_p} for one engine out   .01209

Four major airplane variables were considered in the parametric study to optimize the wing configuration. They are:

1. Wing area
2. Wing aspect ratio
3. Fuel weight
4. Take-off weight

In the study, for each performance goal, the limiting aspect ratio versus wing area is plotted for several take-off weights, including the effects of wing geometry on wing weight. These limits for each of the performance goals are then summarized on a graph so that the best compromise can be selected. A design point of 15.33 square meter (165 square feet) wing area and an effective aspect ratio of 10 were selected.

Table I summarizes the expected weights for fuel, structure-plus-propulsion, and complete aircraft with payload for both conventional and QCGAT aircraft designs.

The first line represents a hypothetical aircraft of current vintage design with low bypass turbofan propulsion. Introduction of a QCGAT high bypass turbofan reduces fuel consumption by 22 percent. When this savings is iterated through the aircraft design, structure and gross weight reduce, provid-

ing an additional 5.5 percent in fuel economy. Similar iterations with weight savings from composite materials and supercritical wing result in an additional 4.4% savings in fuel. The combination of engine and aircraft changes provide 32% better fuel economy. The 22% reduction in gross weight permits. the use of a smaller engine with 22% lower thrust and, therefore, lower absolute emissions and noise.

Out aircraft study projected the maximum ranges shown in figure 6 for various payloads. While 1134 kg (2500 lb) is depicted as maximum payload for the aircraft, only 753 kg (1660 lb) is required to accommodate six people with their baggage. At this payload, the achievable range is in excess of 2963 kilometers (1600 nautical miles). Flight conditions are 10058 meters (33,000 feet) and an average flight speed of approximately 0.5 Mach Number.

In our QCGAT aircraft study, landing distance, rather than take-off capability, set the minimum usable airfield length. Introduction of full-span fowler flaps with moderate wing loading results in a very low "landing configuration" stall speed. The 32 meters/sec (62 knots) stall speed compares with 41 - 46 meters/sec (80 - 90 knots) for current typical jet and turbofan aircraft. Since landing distance is proportional to stall speed squared, this low landing speed provides an attractive sea level FAR landing field length of 811 meters (2660 feet).

Figure 7 shows a representative sample of general aviation airfields plotted on coordinates of field elevation and field length. The Beech QCGAT aircraft with full useful payloads has a landing capability consistent with the majority of these fields.

The expected stall speeds promise a very forgiving airplane in the take-off and landing mode where most accidents occur.

The aircraft preliminary design was conducted to establish realistic criteria for noise measurement. Figure 8 depicts the locations for noise measurement, as well as the aircraft and engine conditions at the point of measurement.

Approach noise is measured directly below the flight path 1852 meters (one nautical mile) prior to the beginning of the runway. Approach aircraft glide slope is fixed at three degrees. Take-off sideline consists of multiple measurements 463 meters (0.25 nautical miles) to one side of the take-off flight path. Take-off flyover condition is measured 6482 meters (3.5 nautical miles) from brake release, directly below the flight path.

Looking at the tabulation of aircraft and engine conditions, the approach conditions are quoted for 40-degree wing flap angle. This gives the shortest landing distance and the highest noise level. Where increase runway length is available, 16 degrees flaps could be used. Velocity would increase to 55.6 meters/sec (108 knots) and thrust would reduce to 818.47 n (184 lb)/engine providing further reduction in noise.

Where take-off sideline noise is measured at multiple locations, the altitude of 262 m (860 ft) produces the highest estimated noise. Conditions are summarized for this altitude.

Climb rate of the QCGAT aircraft approximates current aircraft of similar mission. It attains an altitude of 106 m (3630 ft) at the take-off flyover measurement point.

ENGINE DESIGN

This portion of the paper will touch on design objectives, noise, and emission considerations, engine cycle and engine description, and conclude with specific design features.

Before proceeding into the details of the engine design, a brief review of the design objectives is in order.

> The ecological characteristics of an aircraft system are a direct reflection of the engine design. Careful attention to engine design details which impact noise and emissions is required to produce an engine that will become a welcome resident in a suburban community.

> Appeal of turbofans is indisputable. They swept virtually the entire commercial carrier market in a period of twenty years. The same trend has started in general aviation with the larger size aircraft. The rate of turbofan penetration into the smaller general aviation aircraft size is a function of the engine cost. This cost generally equates to simplicity of engine configuration. The result is basic; to be successful, it must be simple in configuration. Take-off thrust should be sufficient to permit operation from the majority of general aviation airfields.

> The mechanical design life goal should reflect the anticipated aircraft mission. Beech projected a useful aircraft life of 12,000 hours with an average flight cycle lasting 90 minutes. Our design goal was to match this life without replacement of major parts.

> Despite the best intentions of the designer, parts do break and it is desirable to be able to replace them conveniently. Modular engine construction achieves this goal.

> A 12.191-meter (40,000-foot) flight envelope is attractive for avoidance of traffic and bad weather.

> The need for fuel economy goes without saying.

The larger engines for commercial carrier aircraft have demonstrated substantial advances in the technology of noise reduction. They have provided the recipe for quiet engine design which was used for QCGAT and is summarized in figure 9.

Blend low fan blade tip speed and low fan pressure ratio with high fan bypass ratio.

The fan stator should be set at least two fan blade chord lengths aft from the blade trailing edge. The quantity of fan stator vanes should exceed two times the number of fan blades to avoid interaction of fan blade wakes with the stator vanes. Canted stator vanes are preferred.

Exhaust noise reduces with exhaust velocity, and turbine blade-pass frequency should exceed the audible range.

During the iterations which optimize an engine performance cycle, continuous attention is required to avoid adverse impact on emissions characteristics. Table II summarizes the primary causes for emissions along with the engine parameters which have a beneficial influence on emissions.

Unburned hydrocarbons and carbon monoxide emissions are primarily a reflection of poor combustor efficiency at idle. Low combustor inlet temperature at idle aggravates the carbon monoxide emissions. To reduce these two constituents, one would strive for very high combustor efficiency at idle combined with elevated combustor inlet temperature. To achieve the higher inlet temperature, a compressor with poor efficiency at low speed if desired. This compressor should then be run as fast as idle thrust constraints will permit, and then bleed air to achieve even higher speed for the same thrust.

Whereas idle conditions have the primary influence on UHC and CO, take-off conditions predominate in the creation of NO_x. Generally, the higher the combustor inlet temperature at take-off, the more difficult the problem with NO_x. Another important axiom, NO_x and CO can usually be traded through combustor design modification. Either emission can be improved at the expense of the other to achieve the desired combination.

Comments, so far, have ignored engine bypass ratio. Emissions are produced exclusively in the core engine. The higher the bypass ratio, the lower the emissions for a given thrust rating.

A high-pressure compressor pressure ratio of approximately 10/1 under cruise conditions was selected as being achievable without compromise in configuration simplicity. Demonstrated component technology indicated two transonic axial stages combined with a single centrifugal stage would be sufficient. Modest work input requirements for this compressor permit selection of a single-stage air-cooled turbine drive.

An NO_x emission goal was considered the most difficult to achieve, with high-pressure ratio engines requiring a complex combustor configuration. Because NO_x emissions increase with pressure ratio, this 10/1 pressure ratio selection also favored combustor configuration simplicity.

Figure 10 shows the results of one of many parametric performance studies conducted during the cycle selection phase. This particular study was conducted for 7620 meters (25,000 feet) cruise at 0.6 Mach Number. Engine performance is plotted two ways for comparison. The chart on the left provides bare engine performance as it would be measured in an altitude test chamber. The righthand chart modified the SFC coordinate to reflect installed specific fuel consumption. Here, losses associated with nacelle drag and weight are factored in as the nacelle size varies with engine bypass ratio.

Performance for a variety of fan bypass ratios are plotted on coordinates of specific fuel consumption and fan pressure ratio. In both figures, specific fuel consumption is seen to reduce with increasing fan bypass ratio up to a ratio of 10/1. Optimum fan pressure ratio decreases with increasing bypass ratio.

A fan bypass ratio of 9.6/1 at cruise was selected to limit required input work to the capability of a single-stage fan drive turbine. The corresponding fan pressure ratio was set at 1.35.

The engine was sized to produce in excess of 7117 N (1600 lb) of thrust under sea level static operating conditions. Sea level and altitude performance are summarized in table III. This performance compares favorably with even larger, more sophisticated engines currently in use.

Figure 11 schematically shows the engine configuration we selected. The gas generator section was not funded by the NASA QCGAT Program. The engine has only six rotating cascades in total, and only two in the hot section where maintenance costs normally accrue. As such, it achieves the simplicity necessary to penetrate the medium aircraft size general aviation cost barrier.

The configuration is a high-bypass turbofan composed of a single-stage fan, a gas generator section, and a single-stage, low-pressure, fan-drive turbine.

Initial compression is provided by the fan stage with the majority of the air bypassing the gas generator section to produce thrust directly, much as a small propeller would. Air flowing through the hub of the fan enters the gas generator and is further compressed by the high-pressure compressor.

A reverse-flow annular atomizing combustor accommodated fuel burning and energy release. Hot gases take a second 180 degree turn before flowing through the high-pressure compressor-drive turbine.

These gases then continue axially aft through the fan-drive turbine. Power from this turbine is transmitted forward by a shaft that is concentric within the hollow gas generator shaft. Rotational speed is reduced by a reduction gear to match the optimum fan engine.

The advantages of the selected configuration are numerous. Initial studies projected attractive specific fuel consumption while maintaining the desired simplicity of only six rotating cascades. Compliance with the recipe for low noise and emissions has been achieved. The reverse-flow combustor permits packaging the gas generator turbine inside the combustor to achieve a short coupled engine, thus avoiding difficulties of casing deformation and shaft natural frequencies. The resulting engine center-of-gravity is close to the axial plane of the main engine mounts, simplifying installation requirements.

Use of the reduction gear permits individual speed optimization to achieve the best efficiency for the fan and the single-stage low-pressure turbine. Also, the low-pressure turbine may then operate at higher rotational speeds where blade pass frequencies, a common noise source, are outside the audible tone spectrum even under low-speed aircraft approach conditions.

Overall, engine configuration is shown cross sectionally in figure 12. External dimensions are approximately 610 mm X 910 mm (2 feet X 3 feet), not including the accessory gearbox.

Helical reduction gearing introduces an axial mechanical load which opposes aerodynamic loads on both the fan and the low-pressure turbine. This provides a significant reduction in thrust loads on the ball bearings in both the fan and low-pressure turbine rotor systems.

The accessory gearbox is chin-mounted at the bottom of the main frame for ease of maintenance without core cowl removal. Accessory drive is provided from the high-pressure rotor spool via a conventional bevel gear mesh and through-shaft with intermediate bearing support.

Figure 13 shows the modular maintenance features of the engine. The engine disassembles into four basic modules, as shown. The fan module includes fan, stators, reduction gear, and main engine frame. The core module contains the high-pressure compressor, its drive turbine, and the combustor.

Separation of the gas generator and low-pressure turbine modules allows visual inspection of all the hot-section components. Full disassembly of both modules was demonstrated to NASA representatives during the short period of a coffee break at one of our coordination meetings.

On the wing maintenance is virtually unlimited by engine configuration. Hot-section inspection, fan blade accessory replacements, gas generators and low-pressure turbine module exchanges are but a few of the options available to the operator.

The QCGAT engine fan module is depicted in figure 14. The fan blade tip diameter is approximately 559 mm (22 in.) with a modest tip speed of 335 meter/second (1100 feet/second) at take-off conditions. The ratio of stator vanes to fan blades is 2.46 for acoustic considerations. The distance between the fan blade trailing edge and the fan stator vane leading edge has been maintained at 2.1 fan blade chord lengths to minimize noise from rotating blade wakes. The fan stator is canted aft to maximize this distance for a given engine length.

The reduction gear permits high turbine rotational speed producing a blade-pass frequency which is above the audible range, even under reduced power approach conditions.

Fan blade containment capability has been provided in the fan shroud design. Imbalance resulting from blade loss, has been a design criteria for the supporting structure.

Hot oil sprayed into the hub of the spinner provides continuous anti-icing and additional oil cooling.

Figure 15 shows an assembled fan wheel. There are 24 rugged long-chord fan blades which are designed to withstand bird impact without the support of a mid-span shroud. Fewer, long-chord blades were selected as being preferable to a higher quantity of short-chord blades incorporating midspan dampers. This reduces wheel cost and avoids the performance penalties associated with midspan shrouds.

Figure 16 depicts the fan bypass stator assembly. In this design, the stator vanes are manually inserted into potted boots retained in the inner and outer shrouds. This feature permits individual vane replacement rather than returning the entire assembly for overhaul repair in the event of foreign object damage.

The QCGAT main structural frame is shown in figure 17. The frame is integrally cast of aluminum. Four engine mounting bosses are provided to permit selection by the airframe designer for top, side, or bottom engine mounting.

A cross-section of the QCGAT core engine is shown in figure 18. The compressor and turbine stages are mounted on a hollow shaft which acts as a throughbolt furnishing the necessary clamping force for the rotor system.

The compressor rotor thrust load is carried by a ball bearing at the front end. A spring-loaded ball bearing at the end of the shaft permits expansion while maintaining radial position. Accessory drive is taken from this rotor by means of a bevel gear drive.

Two ball bearings, supporting the fan-drive turbine rotor, are contained in the same housing which supports the aft high-pressure rotor bearing. This avoids the cost of lubricating and sealing individual packages. A concentric drive shaft through the high-pressure rotor delivers the fan-drive turbine power to the fan module.

All rotating cascades for both the high-compressor and low-pressure turbine rotors are integrally cast to reduce cost. Air cooling is confined to the high-pressure turbine.

Blade loss containment is provided throughout.

The combustor is a folded annular atomizing burner.

In a conventional atomizing combustor, an axial vortex is generated around each atomizer by swirling the air with vanes. In the QCGAT size combustor, sixteen atomizers and swirlers would have been required to attain even, circumferential, temperature distribution.

Figure 19 shows the "circumferentially stirred" configuration which was selected in preference to the conventional combustor. Primary air is admitted through slots in the liner header producing flow circulation in a circumferentially oriented vortex. Secondary air jets, called "folding jets", enter the inner wall directly downstream of each atomizer and force the circumferential vortex into a horseshoe shape as it flows downstream. In this manner, two downstream vortexes are created for each atomizer, and the required number of atomizers is cut by one-half, to eight.

Prior testing has shown this configuration to be superior to conventional combustors in emissions characteristics. It also demonstrated significant margin in UHC and CO but was initially somewhat above QCGAT NO_X goals. This permitted the trade-off of CO for NO_X mentioned previously to assure achievement of NO_X goals.

As a result of this intensive design effort, the first QCGAT engine was assembled in October 1978. In figure 20, the core engine module is shown being connected to the fan module. Figure 21 is a front 3/4 view of the basic engine fully assembled. The addition of the test inlet bellmouth, plus the core engine cowling, is depicted in figure 22.

Figure 23 shows the birth of a new engine model installed in the test cell just prior to its initial test run. Figure 24 is an enlarged view of the engine installed. The first engine run was in October 1978. A 30-hour mechanical verification test was completed in April 1979. May and June were devoted to damping an undesirable resonance in the ring gear. Emission tests were conducted in July.

Figure 25 shows the engine at the acoustic test site during the acoustic testing phase of the program, which was completed in August. The demonstrator engine was then inspected, acceptance tested, and delivered to NASA in October 1979.

NACELLE DESIGN

A preliminary design in the flight nacelle was defined to establish a realistic baseline from which a ground test nacelle could duplicate the important features at reduced program cost. Only the ground test nacelle was fabricated.

An artist's conception of the flight nacelle is shown in figure 26. The nacelle is composed of the following sections:

1. An inlet duct to provide uniform flow into the engine

2. A fan outer duct and core cowl to guide the bypass air around the engine

3. A mixer assembly to force the mixing of hot, higher velocity core engine exhaust with the cooler, low velocity fan stream

4. A confluent mixing chamber preceding the final nacelle exit nozzle

5. An aerodynamically shaped outer skin, designed to minimize drag at the higher flight speeds.

A mixed-flow confluent exhaust system was selected because it reduces the peak exit velocity, improves propulsive efficiency, and reduces jet noise.

Noise attenuation treatment in the form of perforated acoustic panels has been introduced in the air intake section and in the fan duct outer wall.

Figure 27 shows the engine/nacelle mounting and maintenance access panels. The engine is designed to carry the nacelle aerodynamic and "G" loads. An airframe or nacelle yoke attaches to two points on the engine main frame plus an aft steady link. The entire nacelle is then carried by the appropriate engine flanges. Four access panels are provided for ease of maintenance.

The nacelle aerodynamic contours, summarized in figure 28, are optimized for low drag at 0.65 Mach Number, 10688-meter (35,000-foot) cruise conditions. The intake is designed for high cruise efficiency with modest compromises for static 20.6 meters/sec (40-knot) crosswind tolerance and pressure recovery at low-speed take-off conditions. A NASA/McDonnell-Douglas computer program for three dimensional flow calculations has been used for predicting inlet cowl flow conditions. This program computes flow over axisymmetric bodies at various flow angles of attack. Inlet and fan duct flow velocities are generally below 0.4 Mach Number.

The nacelle is circular in cross-section except for the bottom portion which expands into an elliptical section to house the engine accessories. Boat tail angles vary from 14 to 18 degrees.

The QCGAT ground test nacelle which was used to explore noise and emissions reduction is shown in figure 29. The internal flow lines, flight inlet lip, and the exhaust nozzle are identical to the flight nacelle. External skin was eliminated to reduce program cost.

Flight-worthy hardwall and noise attenuation panels can be readily exchanged as desired.

Three inlet lip configurations (figure 30) which were tested with the QCGAT engine are as follows:

1.   An inlet bellmouth for loss-free baseline calibration

2.   An exact replica of the flight nacelle lip

3.   A lip designed to simulate landing approach inflow conditions.

The flight lip and the inlet bellmouth are compared in figure 31.

Figure 32 shows two views of the mixer nozzle. Studies showed seven lobes to be the optimum for our engine. We selected six, with a very minor performance penalty, to avoid any possible seventh-order upstream excitation of turbine blading. Both shaker tests and engine strain gage testing showed satisfactory dynamic characteristics.

CONCLUSIONS

Challenging objectives were set for the QCGAT aircraft preliminary design to respond to our assessment of general aviation needs for the 1980 decade. The aircraft design achieves these objectives to provide six-place, long-distance flight which will be attractive to both the user and the suburban community.

Flight characteristics of this aircraft have been computed to define realistic criteria for measurement of ecological characteristics.

Reflecting on the engine and nacelle designs, the primary objectives of the QCGAT Program have been fulfilled. Large engine noise reduction technology has been successfully employed to the general aviation size engine. The QCGAT Program culminated in demonstration of QCGAT acoustic goals with margin.

A simplified approach to emissions was conceived in response to this program, and the QCGAT goals for emissions were very nearly achieved. Considerable margin was demonstrated for both CO and UHC emissions and NO_x was within 1 percent of the goal.

QCGAT has given birth to a new engine which is designed to serve the needs of general aviation in the 1980's. While still in its infancy, it has demonstrated attractive performance by current standards. Further development tuning will be required to achieve its full potential which is reflected in

the QCGAT performance goals. Component tests have verified the long term objectives. However, turbine rematch is required to recoup the inherent configuration performance.

Versatile ground test nacelles were created to investigate ecological design parameters. Acoustic panels versus hardwall and mixed exhaust versus split streams were tested under this program.

TABLE I

BENEFITS FROM ADVANCED
AIRCRAFT DESIGN

AIRCRAFT CONFIGURATION	FUEL WEIGHT, Kg (LBS)	STRUCTURE AND PROPULSION WEIGHT, Kg (LBS)	GROSS WEIGHT, Kg (LBS)
Current Aircraft	1,368 (3,016)	2,518 (5,551)	4,518 (9,960)
Introduce QCGAT Engine	992 (2,186)	2,390 (5,268)	4,013 (8,848)
Use Composites and Supercritical Wing	931 (2,053)	1,978 (4,360)	3,538 (7,800)

SAVINGS	32%	23%	22%

TABLE II

DESIGN CONSIDERATIONS FOR EMISSIONS

EMISSION	CAUSE
Unburned Hydrocarbons	Combustion Inefficiency
Carbon Monoxide	Inadequate: Residence Time, Temperature, Efficiency
NOx	High Residence Time/Temperature
Smoke	Local Rich Zones

• Beneficial Engine Characteristics:

    High Combustion Efficiency at Idle

    High Combustor Inlet Temperature at Idle
(High Speed, Low Compressor Efficiency, Bleed)

TABLE III

PROPOSED QCGAT ENGINE PERFORMANCE

| | FLIGHT CONDITION | |
PARAMETER	TAKEOFF Sea Level, Static	MAX CRUISE 0.6 M, 7315 M (25,000 FT)
Thrust	7206 N (1622 lbs)	2162 N (486 lbs)
Specific Fuel Consumption	0.0367 Kg/N/hr (0.360 lb/lb hr)	0.063 (Kg/N hr) (0.626 lb/lb hr)

NEW GENERAL AVIATION AIRCRAFT FOR THE 1980 DECADE
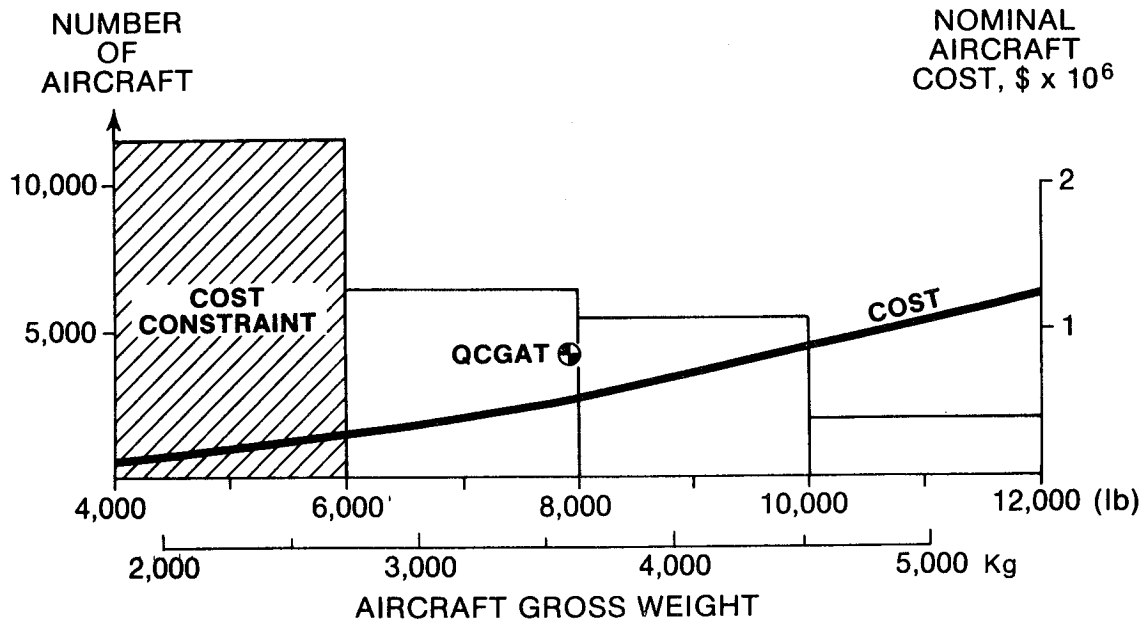
Figure 1

QCGAT AIRCRAFT DESIGN

TWIN FUSELAGE-MOUNTED
QCGAT ENGINES

FULL SPAN/
FOWLER FLAPS

SUPER-CRITICAL WING

WINGLETS

WIDE USE OF
COMPOSITE STRUCTURES

Figure 2

PERFORMANCE
CURRENT AND FUTURE ENGINES

(lb/lb/hr)

Kg/N/hr

JETS AND LOW
BPR FANS

CRUISE
0.6 MACH NO.
9842 M (30,000 FT)

MODERATE
BPR FANS

SFC

*FUEL CONSUMPTION
REDUCED 22%*

QCGAT
HIGH BPR FAN
ADVANCED CYCLE

PERCENT - MAXIMUM THRUST

Figure 3

118
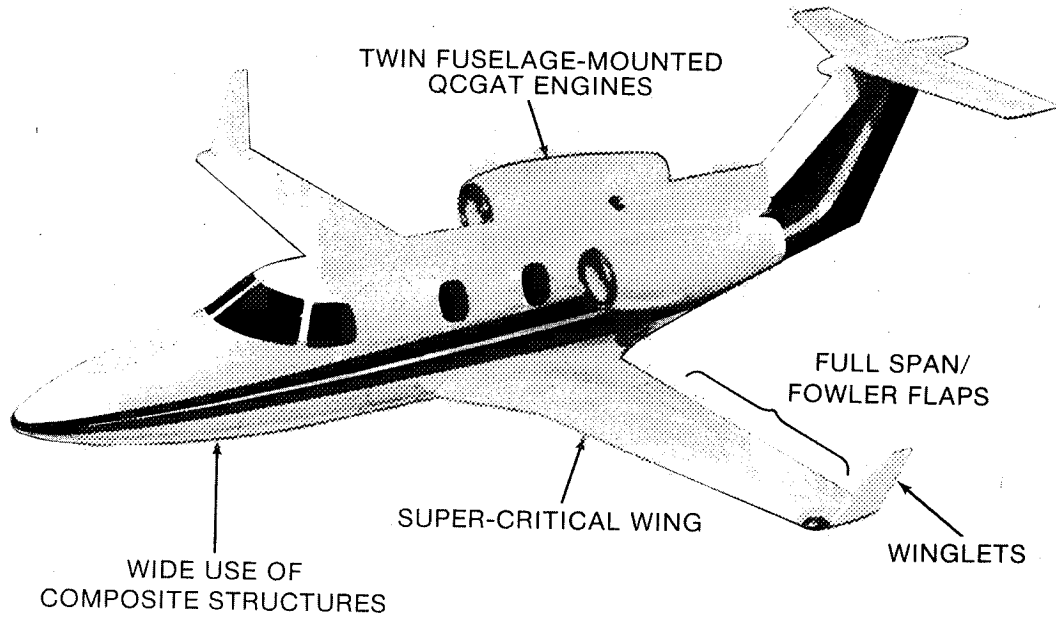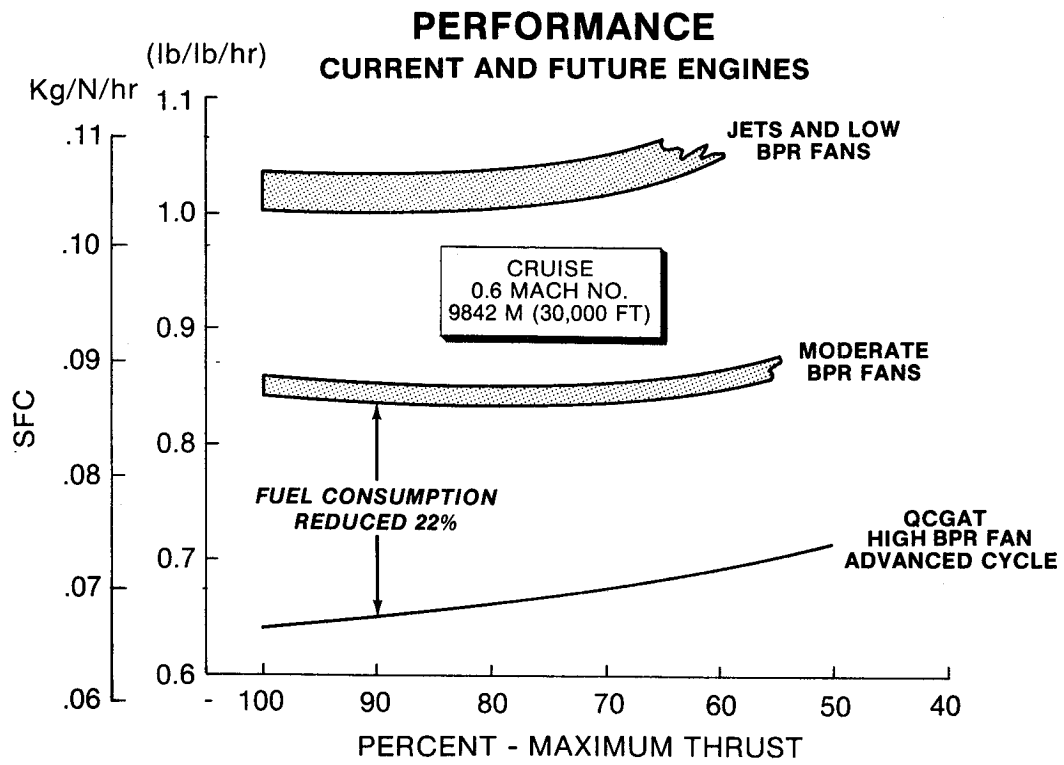
DESIGN AREAS SELECTED
FOR COMPOSITE STRUCTURES

GRAPHITE REINFORCED
KEVLAR SKIN

ALUMINUM SKIN
HONEYCOMB CORE

Figure 4

WING SELECTION

NACA 12%

NASA SUPERCRITICAL 17%

C_D 17% NACA   17% S.C. & 12% NACA

M_N
0.5   0.6   0.7   0.8

PERCENT WEIGHT
+20
+10
0
-10
-20

FUEL CAPACITY   +25%
GROSS WEIGHT   -3%

0.12   0.17
THICKNESS/CHORD

C_L
ΔC_L MAX
35%
17% S.C.
12% NACA

α

Figure 5

119

BEST RANGE vs PAYLOAD

MACH NO. 0.5(MEAN) AT 11,480 M (35,000 FT)
MAX FUEL 975 Kg (2150 lb)

Kg (lb)

PAYLOAD

RANGE

FULL SEATS (6 PEOPLE)
PLUS BAGGAGE
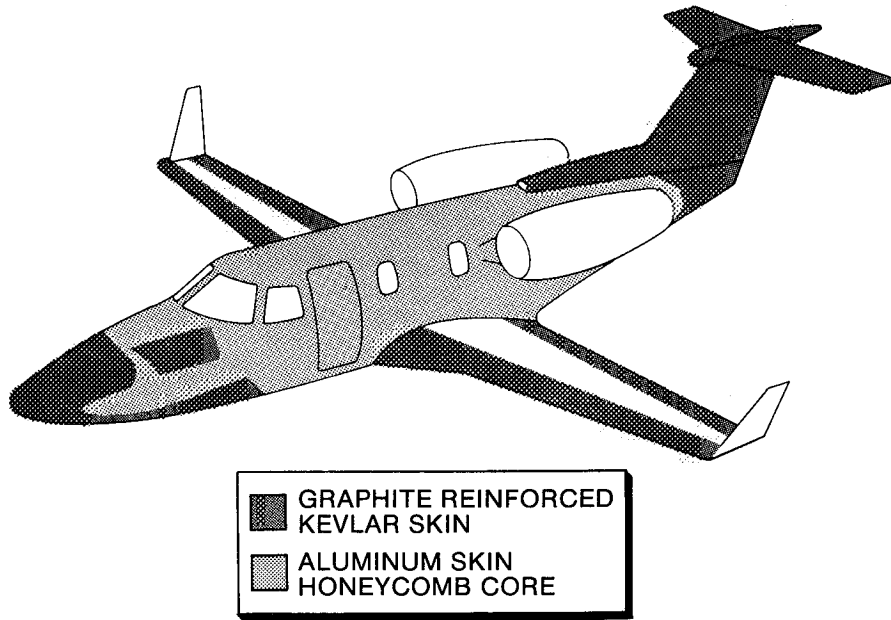
Figure 6

AIRCRAFT STALL SPEED AND FIELD CAPABILITY

M/SEC (KCAS)

STALL SPEED

FLAPS 16°

FLAPS 40°

LANDING
WEIGHT

TAKEOFF
WEIGHT

WEIGHT × 1000

SPECIFIC FIELDS SERVED
BY LOCAL SERVICE AIRLINES IN U.S.A.

Km (FT)

FIELD ELEVATION × 1000

QCGAT

FIELD LENGTH × 1000
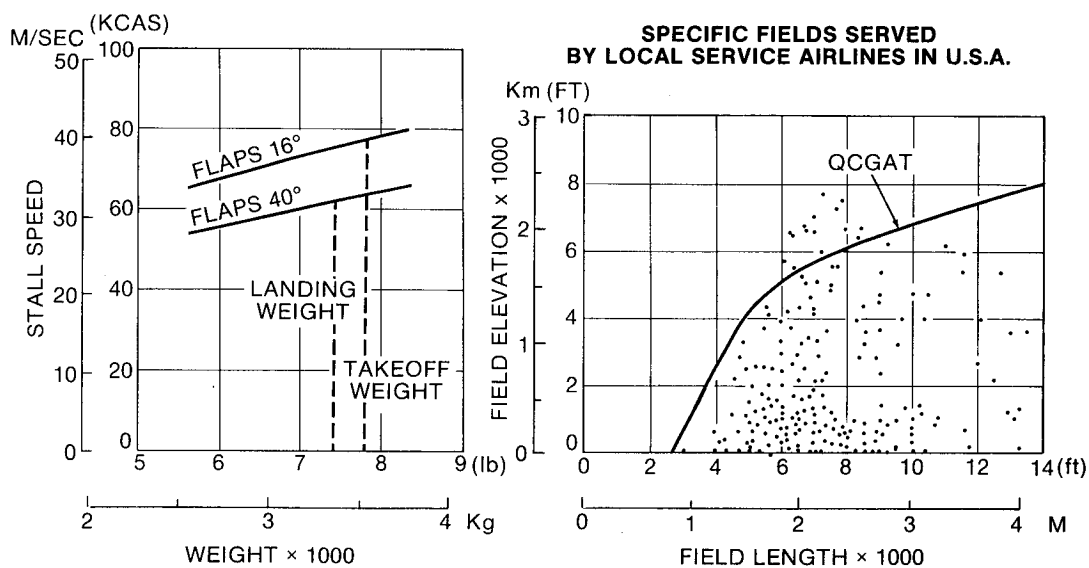
Figure 7

AIRCRAFT NOISE MEASUREMENT CONDITION

CONDITION	ALTITUDE M (FT)	VELOCITY M/SEC (KTS)	THRUST/ENGINE N (LB)	FLAP ANGLE
Approach	113 (370)	46.85 (91)	1157 (260)	40°
Takeoff Sideline	262 (860)	53.02 (103)	4880 (1097)	16°
Takeoff Flyover	1106 (3630)	53.02 (103)	4644 (1044)	16°
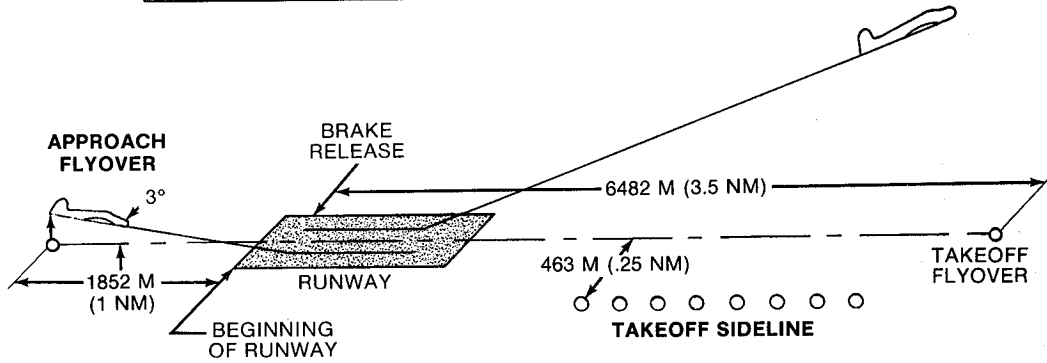
Figure 8

DESIGN CONSIDERATIONS FOR REDUCED NOISE

VANE NUMBER GREATER THAN 2X BLADE NUMBER

HIGH BYPASS RATIO

BLADE PASS FREQUENCY GREATER THAN AUDIBLE

LOW EXHAUST VELOCITY

GREATER THAN TWO FAN BLADE CHORD LENGTHS

LOW TIP SPEED AND PRESSURE RATIO

NO INLET GUIDE VANES

Figure 9

121
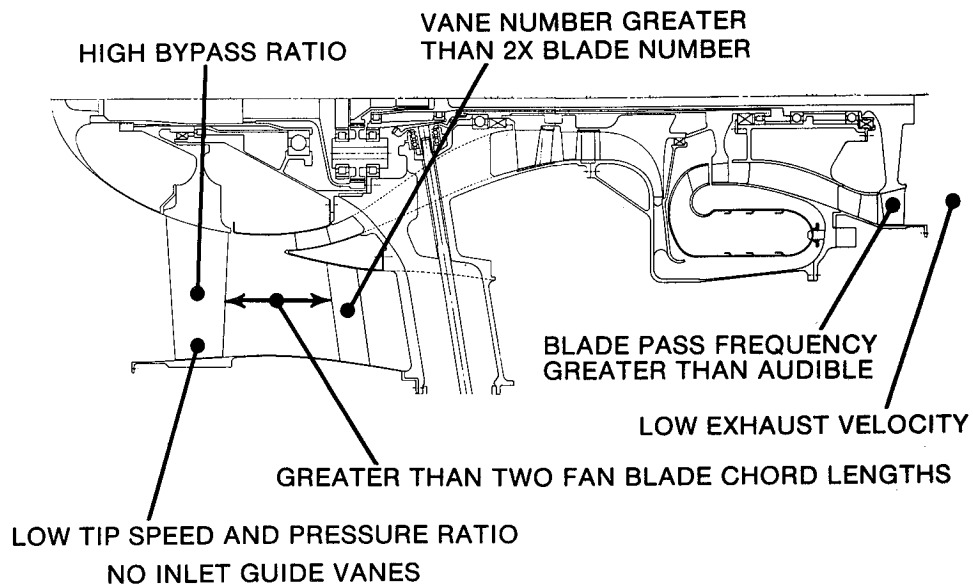
DESIGN STUDY

SAMPLE OF OPTIMIZATION TO DEFINE FAN PRESSURE RATIO

CONSTANT COMPONENT EFFICIENCY
CRUISE AT 0.6 MACH NO. 7315 M (25,000 FT)
ENGINES SIZED FOR CRITICAL OEI
CLIMB OUT AT 0.15 MACH NO.
CYCLE PRESSURE RATIO 10.2

FAN PRESSURE RATIO
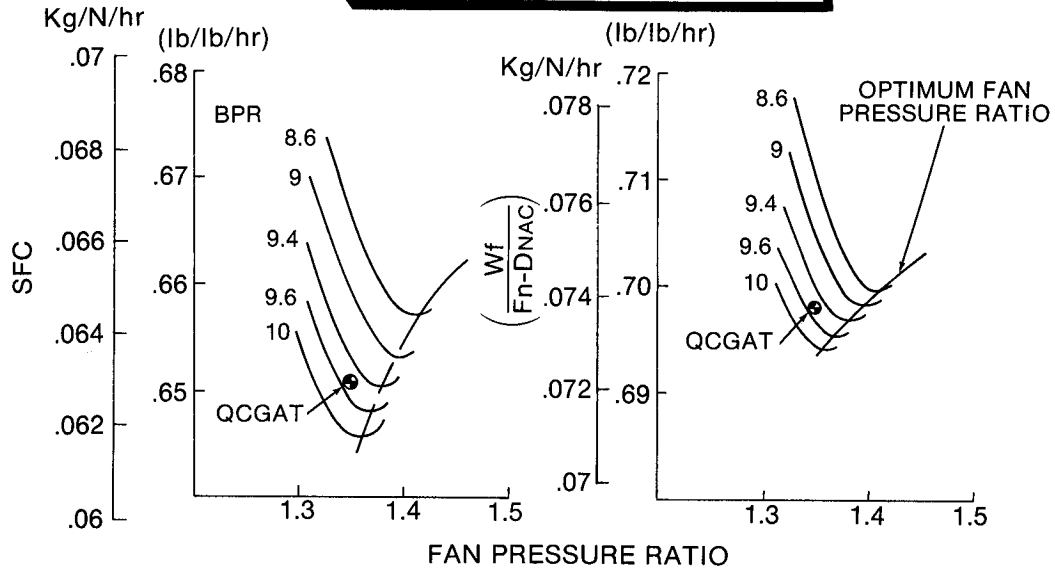
Figure 10

SELECTED QCGAT
ENGINE CONFIGURATION
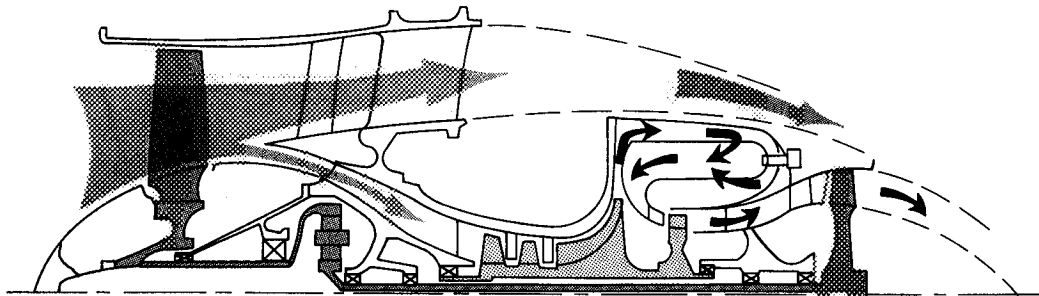
- Configuration Simplicity
  - Six Rotating Cascades
- Superior Performance
- *"GOOD NEIGHBOR"* Design

Figure 11

QCGAT ENGINE CROSS SECTION

891.54 (35.1)

86.36 (3.4)

669.036 (26.3) DIA

609.6 (24.0) DIA

302.26 (11.90) DIA

NOTE: Basic Envelope Dimensions are in mm (inches)

482.6 (19.0)
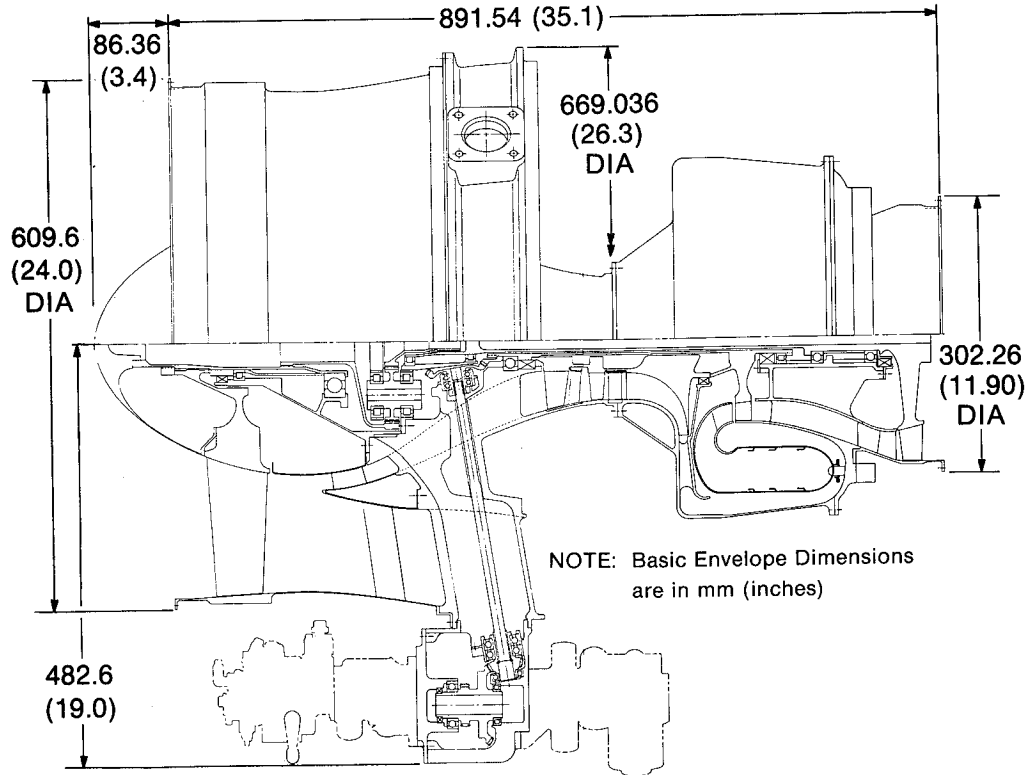
Figure 12

QCGAT ENGINE MODULES

FAN MODULE

GAS GENERATOR MODULE

LOW PRESSURE TURBINE MODULE

ACCESSORY DRIVE MODULE
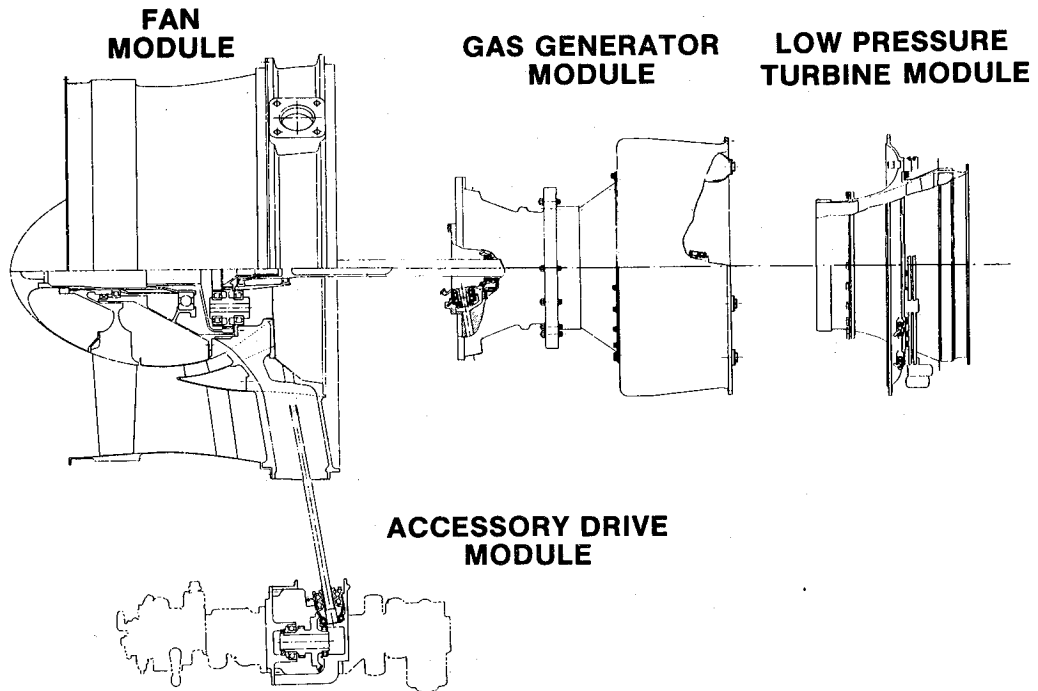
Figure 13

QCGAT FAN MODULE
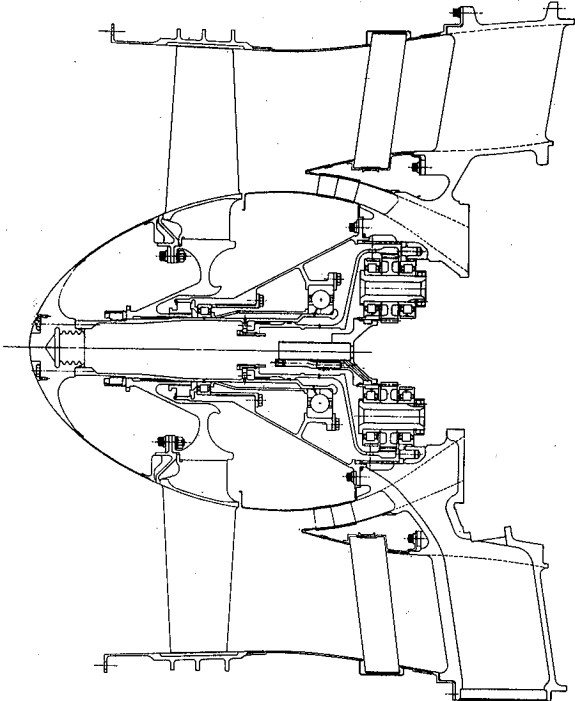
Figure 14

QCGAT FAN WHEEL ASSEMBLY
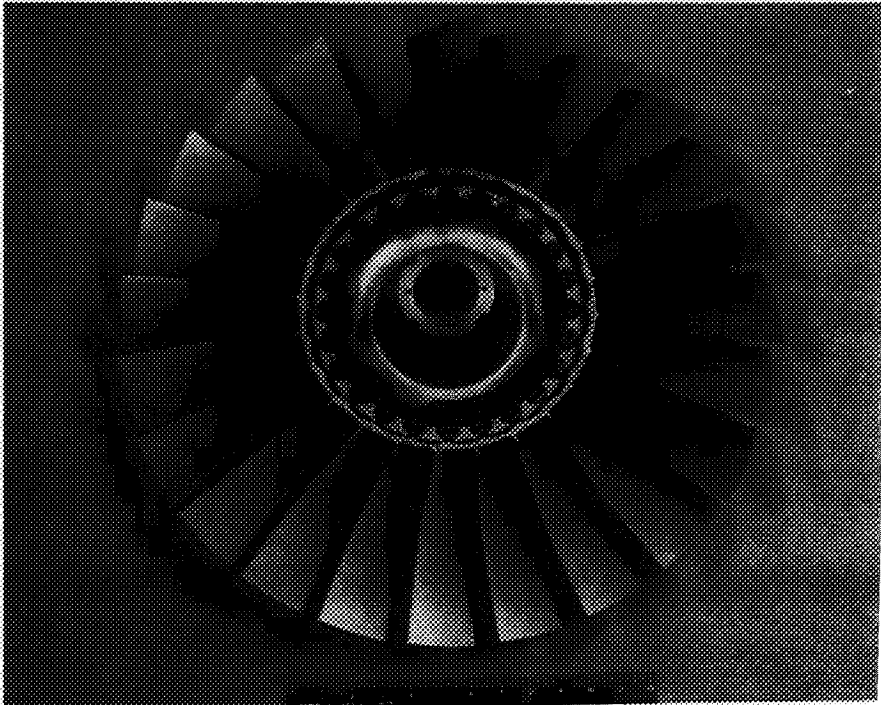
Figure 15

QCGAT REPLACEABLE VANE FAN STATOR
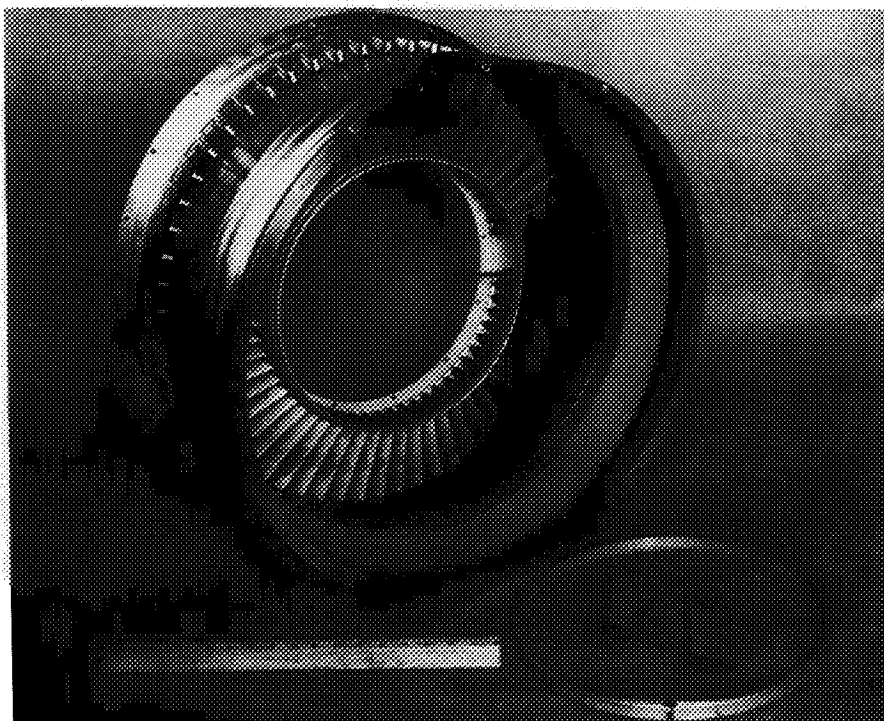
Figure 16

QCGAT ENGINE MAIN FRONT FRAME
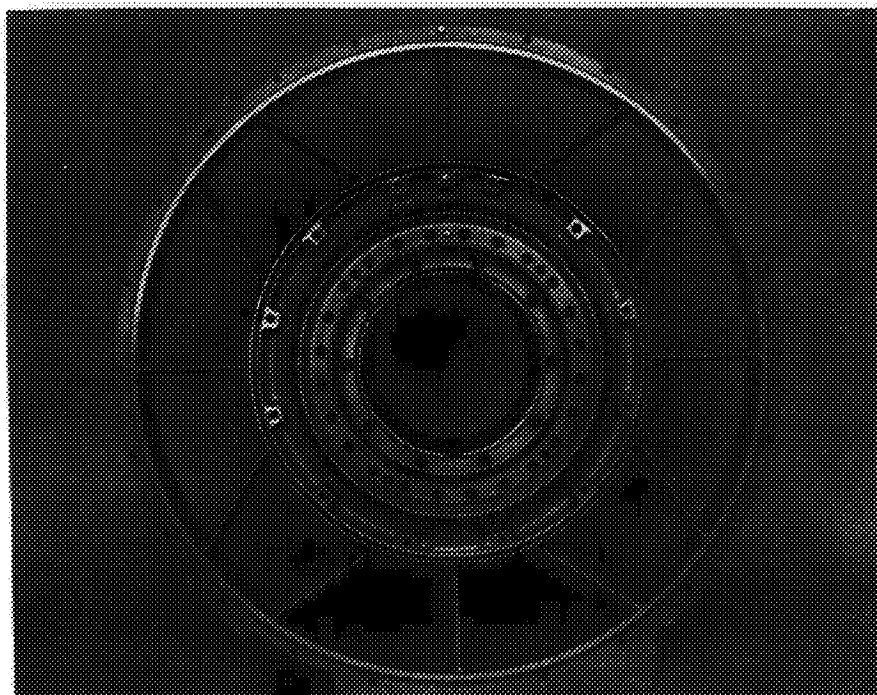
Figure 17

QCGAT CORE ENGINE
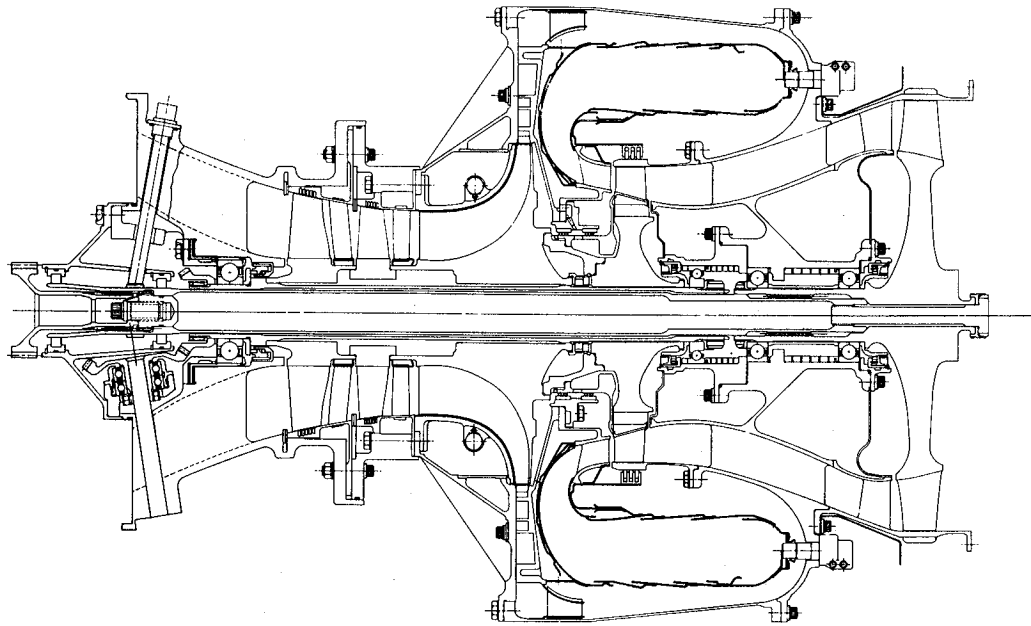
Figure 18

QCGAT COMBUSTOR

MEAN VORTEX
CIRCULATION PATH

SECONDARY
FOLDING JETS

VORTEX
CIRCULATION
PATTERN

VIEW A—A

FUEL
INJECTOR

AIR ENTRY

PRIMARY
ZONE

SECONDARY
FOLDING JETS

Figure 19

126
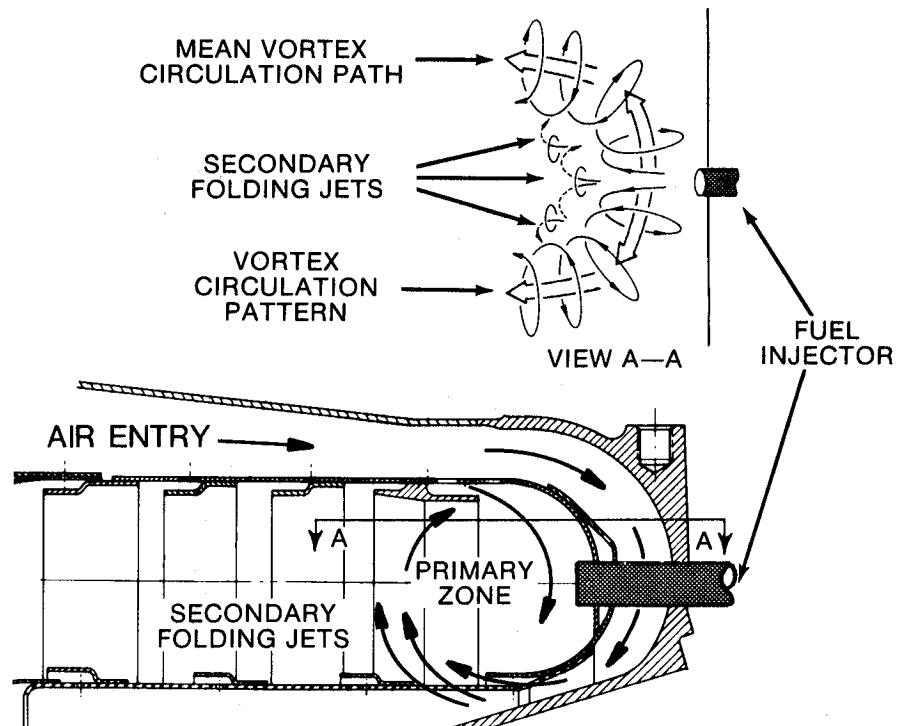
QCGAT ENGINE ASSEMBLY
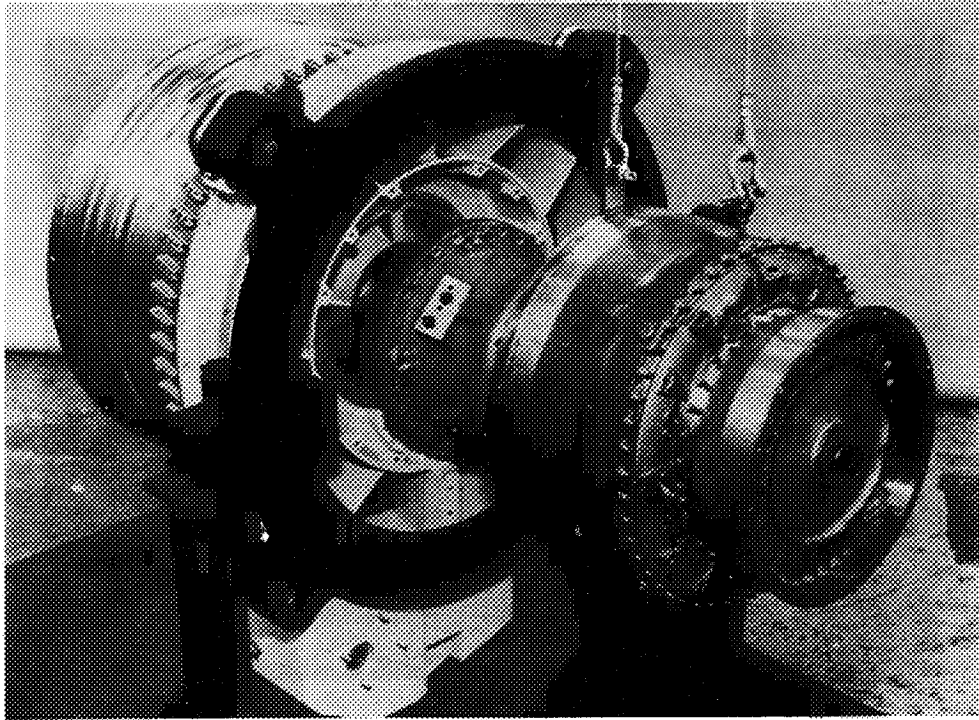
Figure 20

QCGAT ENGINE

Figure 21

127
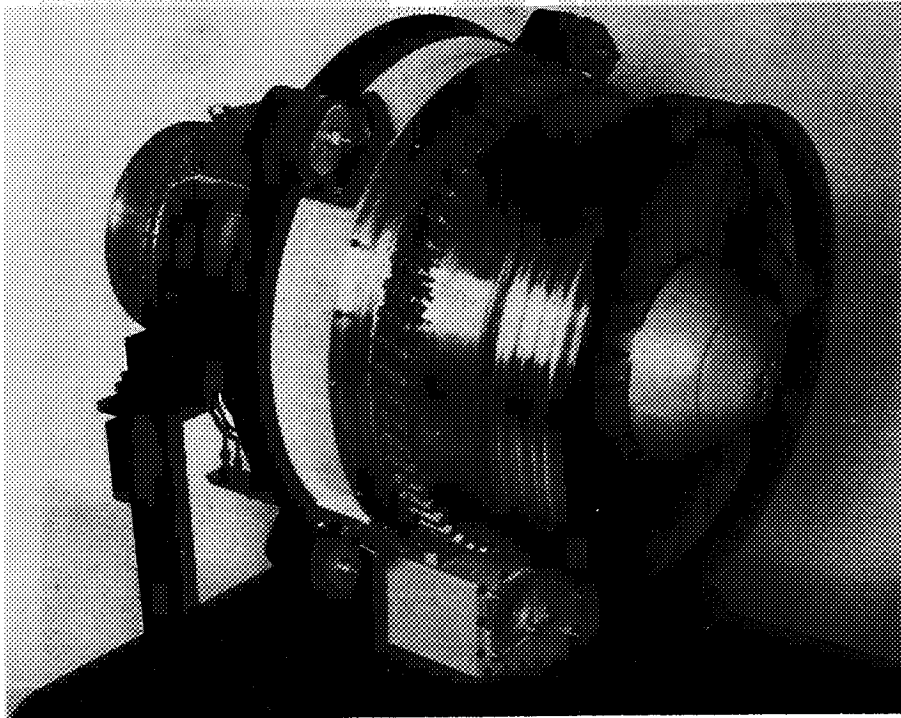
QCGAT ENGINE WITH BELLMOUTH
AND CORE COWL
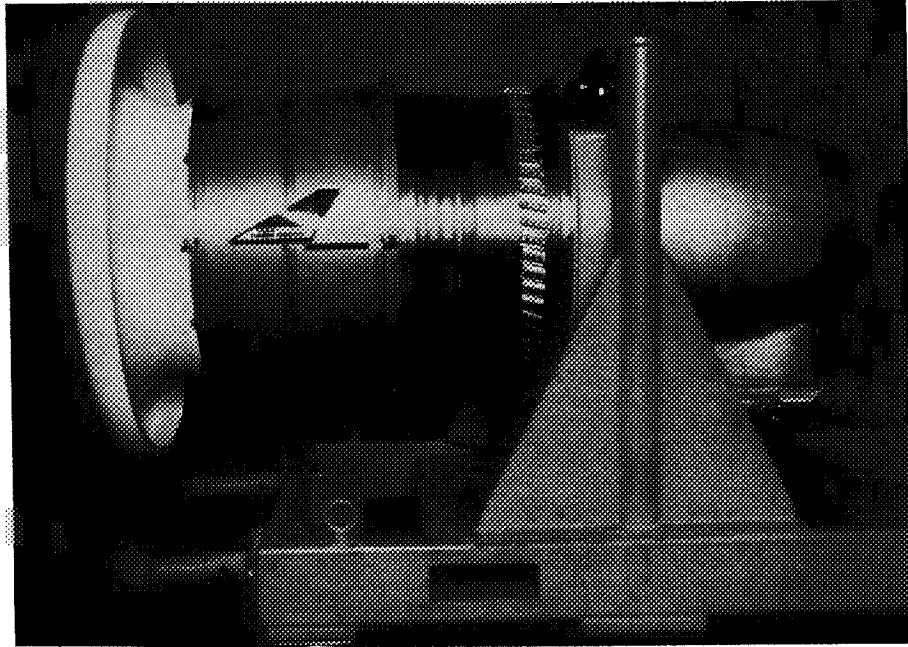
Figure 22

QCGAT ENGINE IN DEVELOPMENT TEST CELL

Figure 23

128
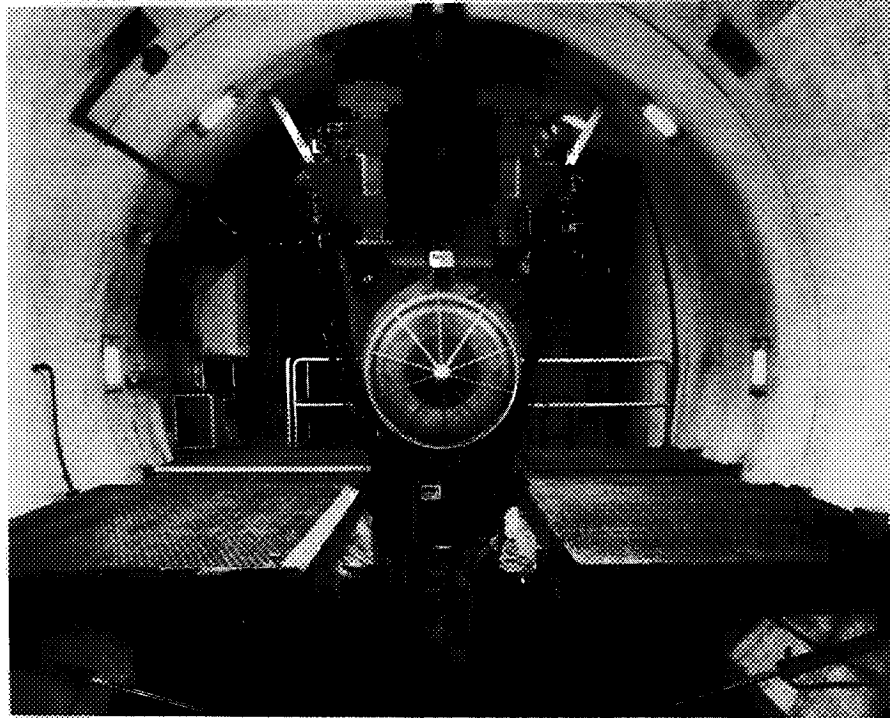
QCGAT ENGINE AT ACOUSTIC TEST SITE
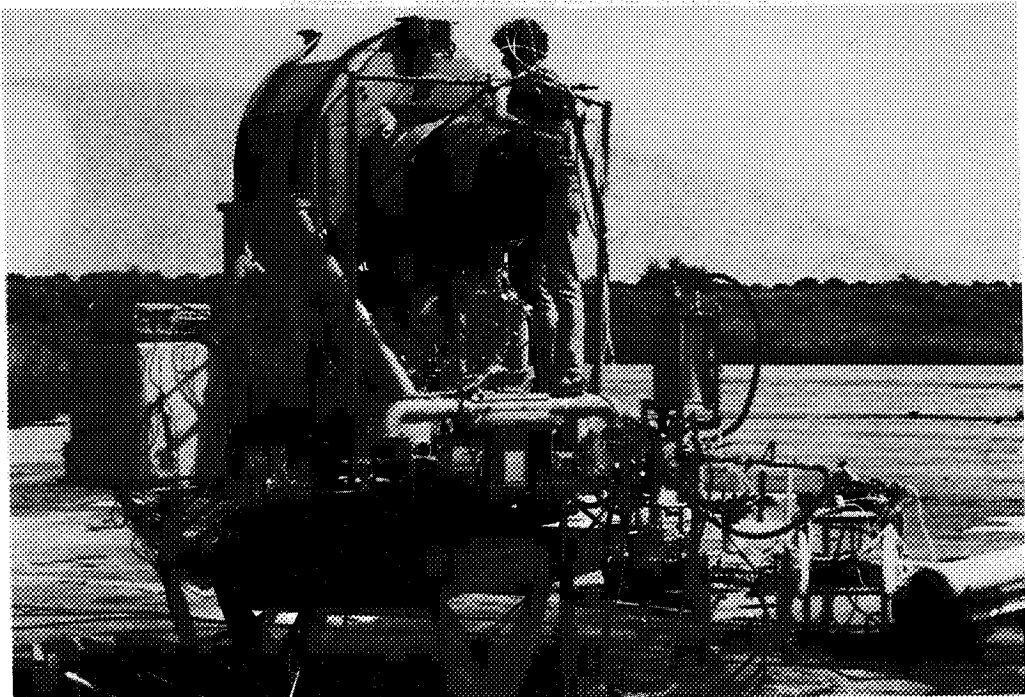
Figure 25

QCGAT ENGINE IN DEVELOPMENT TEST CELL

Figure 24

129
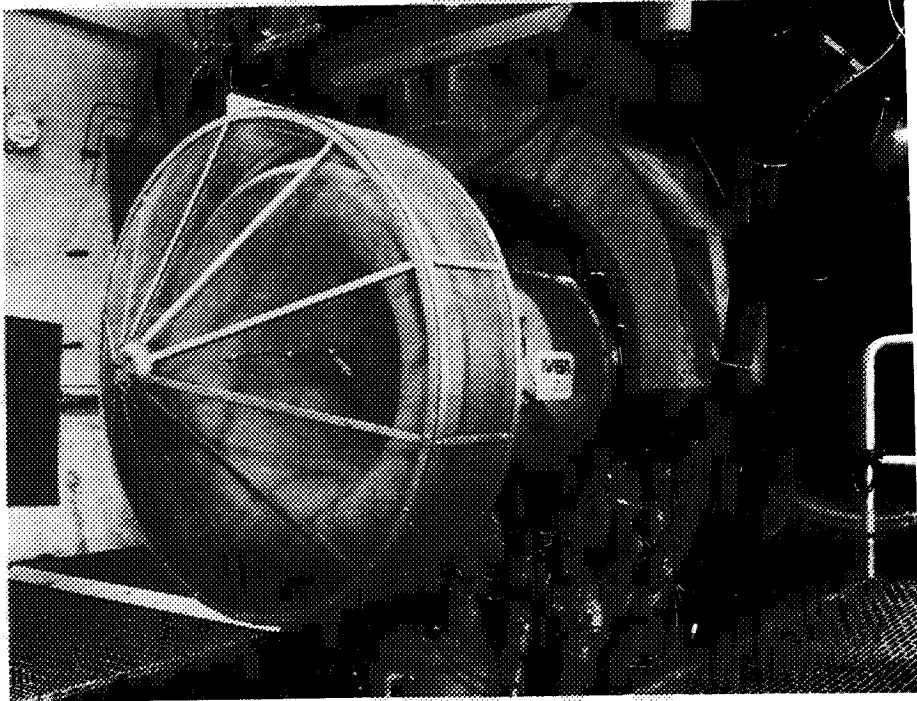
NASA - AVCO LYCOMING
Quiet Clean General Aviation Turbofan
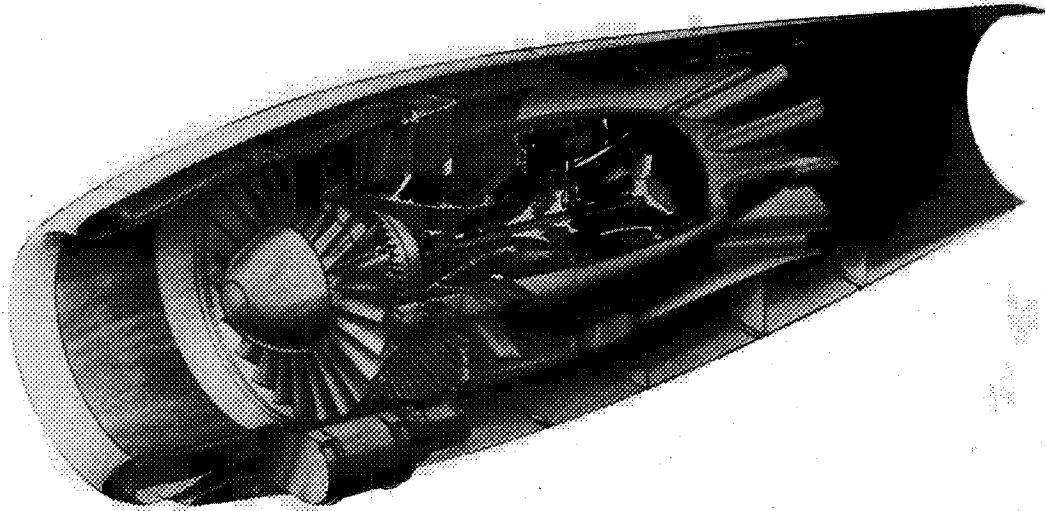
Figure 26

QCGAT NACELLE ACCESS PANELS

TOP
PANEL

BOTTOM
PANEL

SIDE
PANEL

EASY ACCESS
PANEL
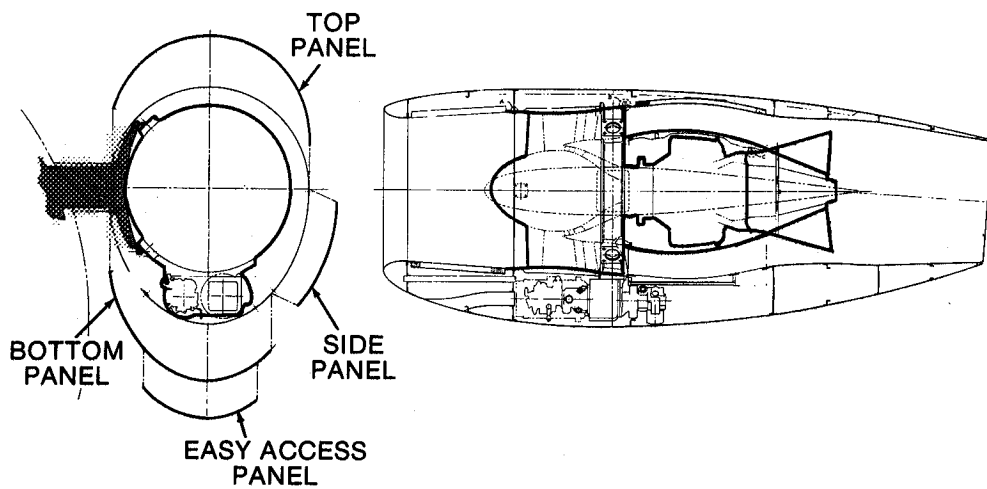
Figure 27

QCGAT NACELLE EXTERNAL GEOMETRY
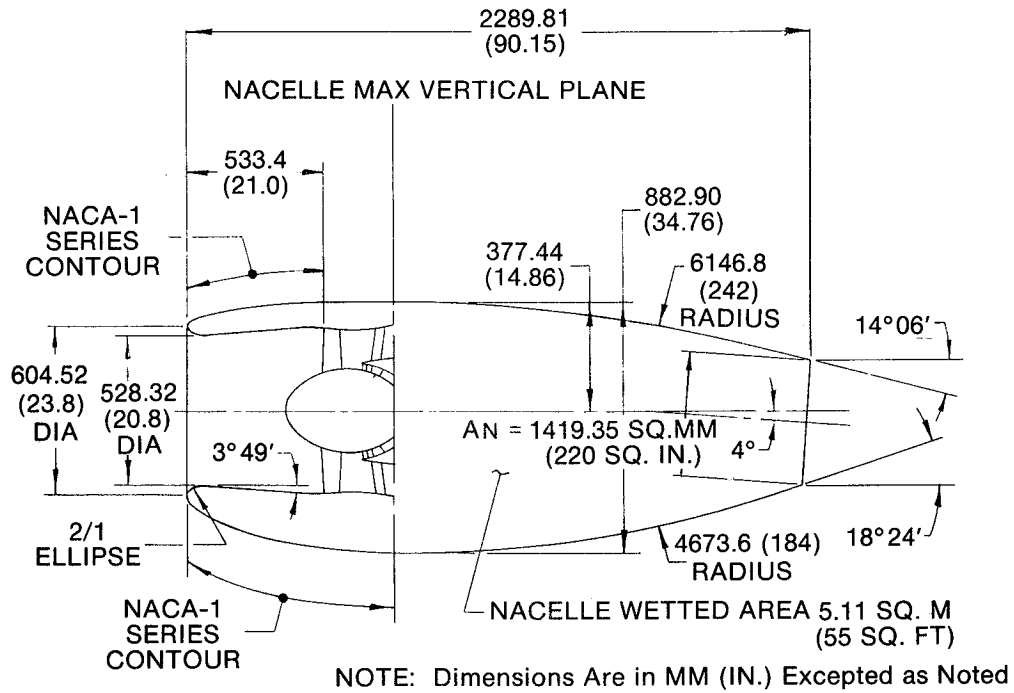
Figure 28

QCGAT FLIGHT NACELLE SIMULATION
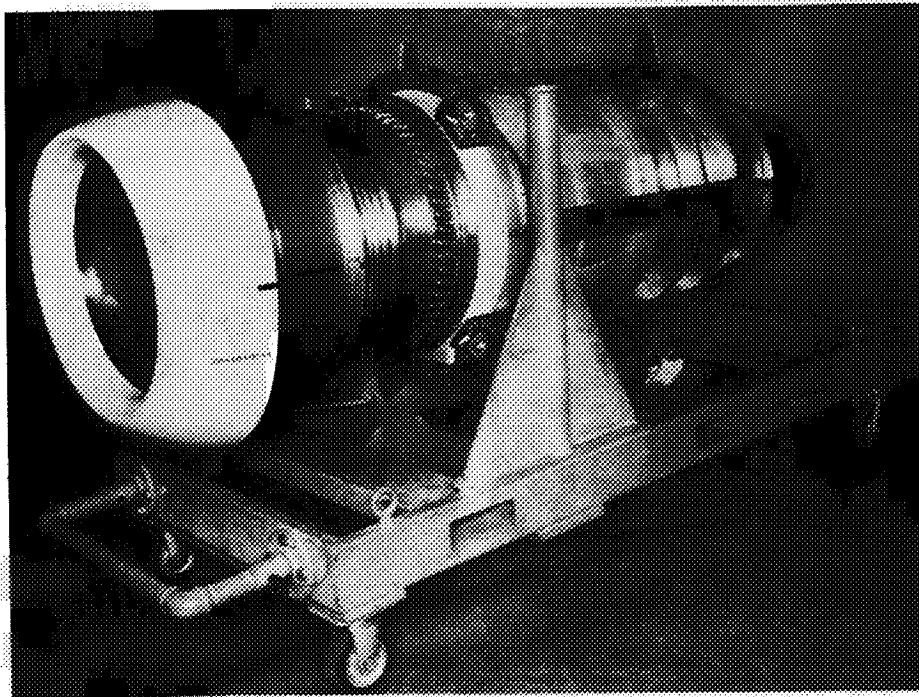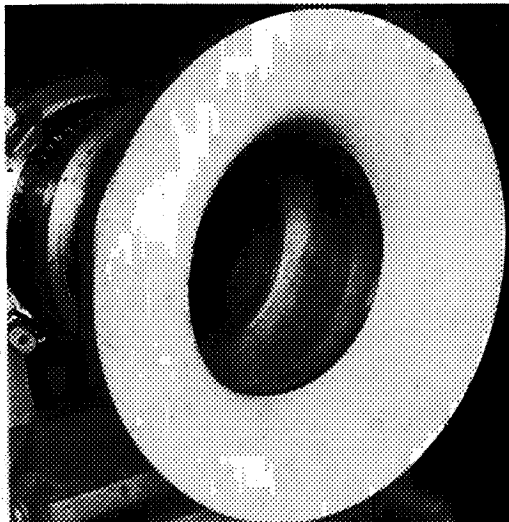

Figure 29

REPLACEABLE INLET LIPS

FLIGHT NACELLE **SYMETRICAL BELLMOUTH** **APPROACH SIMULATOR**
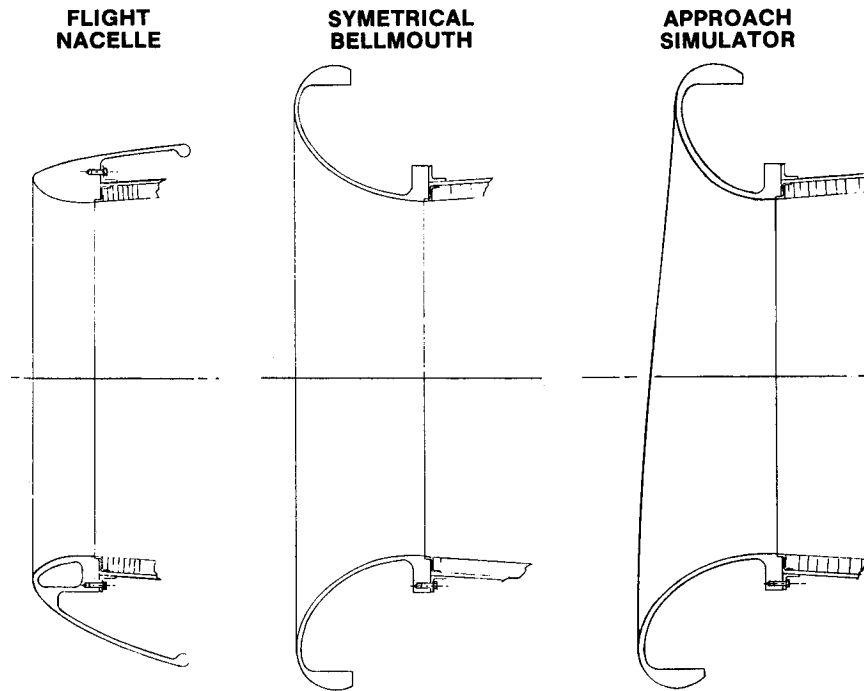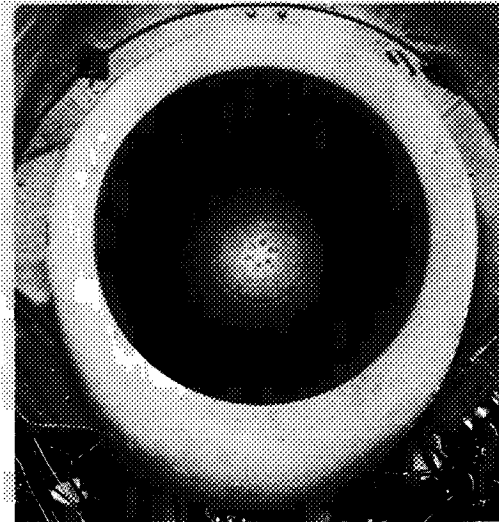

Figure 30

BELLMOUTH INLET   FLIGHT NACELLE INLET

Figure 31

QCGAT MIXER ASSEMBLY

Figure 32